Protein Science (1998), 7:2451–2459. Cambridge University Press. Printed in the USA.

The kinetic cycle of cardiac troponin C: Calcium binding and dissociation at site II trigger slow conformational rearrangements

ANDREA L. HAZARD,[1] SUSY C. KOHOUT,[1] NICOLE L. STRICKER,[1]
JOHN A. PUTKEY,[2] AND JOSEPH J. FALKE[1]

[1]Department of Chemistry and Biochemistry, University of Colorado, Boulder, Colorado 80309-0215
[2]Department of Biochemistry and Molecular Biology, University of Texas Medical School, Houston, Texas 77225

(RECEIVED December 3, 1997; ACCEPTED August 5, 1998)

Abstract

The goal of this study is to characterize the kinetic mechanism of Ca^{2+} activation and inactivation of cardiac troponin C (cTnC), the Ca^{2+} signaling protein which triggers heart muscle contraction. Previous studies have shown that IAANS covalently coupled to Cys84 of wild-type cTnC is sensitive to conformational change caused by Ca^{2+} binding to the regulatory site II; the present study also utilizes the C35S mutant, in which Cys84 is the lone cysteine, to ensure the specificity of IAANS labeling. Site II Ca^{2+} affinities for cTnC-wt, cTnC-C35S, cTnC-wt-IAANS$_2$, and cTnC-C35S-IAANS were similar (K_D = 2–5 μM at 25 °C; K_D = 2–8 μM at 4 °C), indicating that neither the IAANS label nor the C35S mutation strongly perturbs site II Ca^{2+} affinity. To directly determine the rate of Ca^{2+} dissociation from site II, the Ca^{2+}-loaded protein was rapidly mixed with a spectroscopically sensitive chelator in a stopped flow spectrometer. The resulting site II Ca^{2+} off-rates were k_{off} = 700–800 s^{-1} (4 °C) for both cTnC-wt and cTnC-C35S, yielding calculated macroscopic site II Ca^{2+} on-rates of $k_{on} = k_{off}/K_D$ = 2–4 × 10^8 M^{-1} s^{-1} (4 °C). As observed for Ca^{2+} affinities, neither the C35S mutation nor IAANS labeling significantly altered the Ca^{2+} on- and off-rates. Using IAANS fluorescence as a monitor of the protein conformational state, the intramolecular conformational changes (Δ) induced by Ca^{2+} binding and release at site II were found to be significantly slower than the Ca^{2+} on- and off-rates. The conformational rate constants measured for cTnC-wt-IAANS$_2$ and cTnC-C35S-IAANS were $k_{\Delta on}$ = 120–210 s^{-1} and $k_{\Delta off}$ = 90–260 s^{-1} (4 °C) . Both conformational events were slowed in cTnC-wt-IAANS$_2$ relative to cTnC-C35S-IAANS, presumably due to the bulky IAANS probe coupled to Cys35. Together, the results provide a nearly complete kinetic description of the Ca^{2+} activation cycle of isolated cTnC, revealing rapid Ca^{2+} binding and release at site II accompanied by slow conformational steps that are likely to be retained by the full troponin complex during heart muscle contraction and relaxation.

Keywords: calcium signaling; calmodulin; metal binding site troponin C

Cardiac troponin C (cTnC) activates heart muscle contraction in response to a Ca^{2+} signal. As a member of the calmodulin superfamily, cTnC shares strong sequence homology with other eukaryotic signaling proteins, including calmodulin and the skeletal form of troponin C (sTnC), both of which have been described by crystallographic and NMR structures (Babu et al., 1988; Herzberg & James, 1988; Satyshur et al., 1988; Taylor et al., 1991; Chattopadhyaya et al., 1992; Starovasnik et al., 1992; Rao et al., 1993; Finn et al., 1995; Gagne et al., 1995; Kuboniwa et al., 1995; Zhang et al., 1995). Recently, the NMR structure of cTnC was solved by Sykes and coworkers (Sia et al., 1997), confirming the similar overall architecture of the three proteins, in which two structurally independent domains are separated by a flexible linker involved in effector binding. Most members, including calmodulin and sTnC, contain two EF-hand sites in each domain (sites I–IV). The comparatively rare feature of cTnC, however, is that site I does not bind Ca^{2+} because of natural substitutions at coordinating positions. As a result, cTnC possesses site II as the only functional site in the regulatory N-terminal domain, along with sites III and IV in the structural C-terminal domain (van Eerd & Takahashi, 1975; Burtnick & Kay, 1977; Leavis & Kraft, 1978).

Reprint requests to: Joseph J. Falke,Department of Chemistry and Biochemistry, University of Colorado, Campus Box 215, Boulder, Colorado 80309-0215; e-mail: falke@colorado.edu.

Abbreviations: cTnC, cardiac troponin C; sTnC, skeletal troponin C; IAANS, 2-(4′-iodoacetamido-anilino)-naphthalene-6-sulfonic acid.

Numerous studies indicate that site II alone is the Ca^{2+}-trigger site for heart muscle contraction. For example, a peptide fragment of the N-terminal domain containing site II (cTnC 1–88) could restore actomyosin ATPase activity to stripped skeletal muscle fibers, while a peptide fragment of the C-terminal domain containing sites III and IV (cTnC 103–158) could not (McCubbin & Kay, 1985). Furthermore, Ca^{2+} activation is lost when site II is selectively destroyed by mutagenesis (Gulati et al., 1989; Putkey et al., 1989; Sweeney et al., 1990). In contrast, cTnC retains function in myofibril ATPase and force generation assays even when sites III and IV are inactivated, specifically by substitution of alanine for the coordinating sidechains at positions 1 or 3 of both EF-loops (Negele et al., 1992; Dotson & Putkey, 1993). These results demonstrate that site II is responsible for triggering heart muscle contraction, while sites III and IV appear to play a structural role in the docking of cTnC to troponin I of the assembled tropomyosin complex (Zot & Potter, 1982; Negele et al., 1992; Liao et al., 1994). This picture is further supported by the high Ca^{2+}-specificity of site II, which prevents occupancy until a Ca^{2+} signal appears, while sites III and IV exhibit the Ca^{2+}/Mg^{2+}-specificity characteristic of structural or buffering sites (Leavis & Kraft, 1978; Holroyde et al., 1980; Johnson et al., 1980; Negele et al., 1992; Dong et al., 1996).

Previous work indicates that the environment of the cTnC interdomain linker, consisting of residues 84 through 94 (Sia et al., 1997), changes upon Ca^{2+} binding to site II. This is particularly true for the N-terminal region of the linker, as well as the C-terminal end of helix D just preceding the linker. For example, the chemical labeling rates, quantum yields, and lifetimes of fluorescent probes attached to Cys84 at the N-terminus of the linker are each observed to change upon Ca^{2+} binding to site II (Johnson et al., 1980; Putkey et al., 1989; Hannon et al., 1992; Dong et al., 1996, 1997a, 1997b; Dong & Cheung, 1996). Ca^{2+} binding to site II also induces large H_ϵ and C_ϵ chemical shift changes for M80 and M81 on the C-terminal end of helix D, and increases the exposure of M81 to a soluble spin label (Lin et al., 1994; Howarth et al., 1995). Significant NMR chemical shift changes of Met81 upon complexation of cTnC with cTnI further imply that conformational changes in this region of the linker region help regulate interaction of cTnC with its effector (Krudy et al., 1994). We chose to use the fluorescence of the probe 2-(4′-iodoacetamidoanilino)-naphthalene-6-sulfonic acid (IAANS) attached to Cys84 to monitor Ca^{2+}-induced environmental changes involving the inter-domain linker. To prevent IAANS labeling at alternative sites, the engineered isoform cTnC-C35S was constructed to remove Cys35, the only other cysteine in the protein. Conversion of Cys35 to Ser or Ala does not significantly alter the Ca^{2+} affinity of site II and has no detectable effect on the ability to activate myofibril ATPase activity, indicating that conservative substitutions at this position do not perturb site II function (Putkey et al., 1993; Dong et al., 1996).

We describe, herein, a kinetic analysis of Ca^{2+} binding and dissociation at site II of isolated cTnC-wt and cTnC-C35S. This study is the first to directly resolve the kinetics of Ca^{2+} binding and release from the rates of induced conformational changes, both in the activation and inactivation branches of the kinetic cycle. Our results indicate that rapid Ca^{2+} binding and dissociation events at site II are each followed by slower conformational transitions, indicating a two-step mechanism for Ca^{2+} activation and inactivation. The ability of cTnC to undergo such two-step processes has important implications for models of heart muscle contraction, since one must now consider the possibility that Ca^{2+} binding and conformational activation are distinct, rather than simultaneous, events.

Results

Protein purification and IAANS labeling

Protein was expressed in *Escherichia coli* and isolated by standard methodology. The expected molecular weights of 18,256 and 18,240 Da for cTnC-wt and cTnC-C35S were confirmed by electrospray mass spectrometry. Ca^{2+} binding stoichiometries of 2.8 mole per mole protein were determined for both cTnC-wt and cTnC-C35S. When appropriate, protein was labeled with IAANS, an environment sensitive fluorophore which covalently alkylates protein sulfhydryl groups via its iodoacetamide functionality. IAANS labeling stoichiometries, determined by absorbance, were 2.1 mole per mole protein for cTnC-wt and 0.9 mole per mole protein for cTnC-C35S. Since cTnC-wt contains two cysteine residues, Cys35 and Cys84, while cTnC-C35S possesses only the latter, it follows that IAANS labeling proceeds to near completion in each protein.

IAANS fluorescence titrations

It has been shown (Johnson et al., 1980) that the IAANS fluorescence of labeled cTnC-wt decreases by ~10% with Ca^{2+} binding to sites III and IV, and increases by ~60% with Ca binding to site II. More recent studies in which either Cys35 or Cys84 was substituted with serine demonstrate that the IAANS label at Cys84 alone is responsible for this fluorescence change in isolated cTnC (Dong et al., 1996, 1997a, 1997b; Putkey et al., 1997). Ca^{2+} titration profiles obtained here for both cTnC-wt-IAANS and cTnC-C35S-IAANS match those previously described as illustrated in Figure 1 for cTnC-wt. At 4 °C, the extent of the fluorescence decrease becomes larger and the extent of the fluorescent increase becomes smaller, such that the two events become approximately equal in amplitude (data not shown).

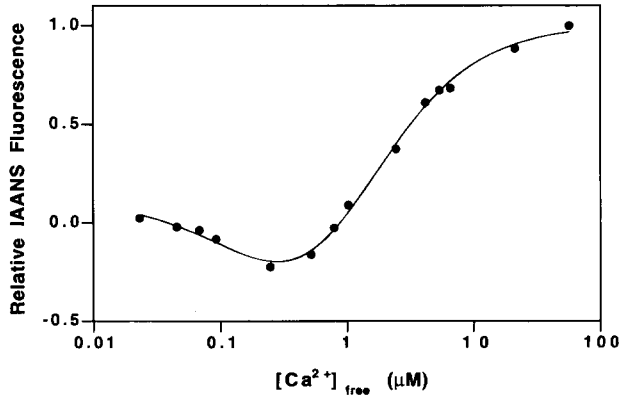

Fig. 1. cTnC-C35S IAANS fluorescence titration. Indicated is the IAANS fluorescence profile obtained by titrating cTnC-C35S-IAANS with $CaCl_2$. The best-fit curve is calculated for a two-component binding reaction in which Ca^{2+} triggers a fluorescence increase for one component (site II) and a fluorescence decrease for the other (coupled sites III, IV; see Equation 3 in Materials and methods). The resulting best-fit Ca^{2+} dissociation constants are $K_{D(II)} = 1.0 \pm 0.4$ μM and Ca^{2+} $K_{D(III,IV)} = 0.3 \pm 0.2$ μM, respectively. Conditions were 90 mM KCl, 10 mM MOPS pH 7.0, 1 mM EGTA, 1 μM protein, 25 °C.

Table 1. *Equilibrium Ca^{2+} binding to site II*

Protein[a]	Temperature (°C)	IAANS Ca^{2+} K_D[b] (μM)	Magnesium green Ca^{2+} K_D[c] (μM)	
		IAANS-labeled	Unlabeled	IAANS-labeled
cTnC-wt	25	3 ± 1	3 ± 1	2 ± 1
	4	5 ± 2	2 ± 1	3 ± 1
cTnC-C35S	25	2 ± 1	5 ± 2	4 ± 2
	4	8 ± 4	3 ± 1	3 ± 1

[a]All samples contained 90 mM KCl, 10 mM MOPS, pH 7.0.
[b]The K_D for Ca^{2+} binding to site II was determined by the IAANS fluorescence assay. Samples contained 1 μM labeled protein and 1 mM EGTA as a Ca^{2+} buffer.
[c]The K_D for Ca^{2+} binding to site II was measured using the Ca^{2+} chelator magnesium green. Samples contained 1 μM protein and 1 μM chelator.

Site II Ca^{2+} affinities

The equilibrium dissociation constant (K_D) for Ca^{2+} binding to site II was determined using two independent methods. First, the site II Ca^{2+} K_D of IAANS-labeled cTnC was determined by titrating the protein with Ca^{2+} and fitting the change in IAANS fluorescence to Equation 3 in Materials and methods (Fig. 1). Second, to ascertain whether the C35S mutation or the IAANS label perturbs the equilibrium Ca^{2+} binding, the site II Ca^{2+} K_D's of both IAANS-labeled and unlabeled cTnC were determined by titrating each protein with Ca^{2+} in the presence of the fluorescent Ca^{2+} chelator magnesium green. The latter method quantitates $[Ca^{2+}]_{free}$ and enables determination of $[Ca^{2+}]_{bound \cdot cTnC}$ by subtraction as described in Materials and methods. The K_D values summarized in Table 1 indicate that the site II Ca^{2+} affinities for cTnC-wt, cTnC-C35S, cTnC-wt-IAANS$_2$, and cTnC-C35S-IAANS are similar to one another (K_D = 2–5 μM at 25 °C; K_D = 2–8 μM at 4 °C), corresponding to variations in binding free energy less than 0.6 kcal mol^{-1}. It follows that neither the C35S mutation nor the IAANS probe strongly perturbs the Ca^{2+} affinity of site II. Similar Ca^{2+} affinities have been previously reported for site II (Holroyde et al., 1980; Johnson et al., 1980; Dong et al., 1997a), although the present results provide the first direct comparison of K_D values between unlabeled and IAANS-labeled cTnC variants. The IAANS fluorescence titrations also determined a macroscopic Ca^{2+} K_D for the higher affinity, tightly coupled sites III and IV (for cTnC-wt-IAANS$_2$, K_D = 0.2 ± 0.1 μM at 25 °C and 0.7 ± 0.4 μM at 4 °C; for cTnC-C35S-IAANS, K_D = 0.2 ± 0.1 μM at 25 °C and 1.3 ± 0.5 μM at 4 °C), again yielding values in agreement with those previously published (Holroyde et al., 1980; Johnson et al., 1980).

Site II Ca^{2+} association and dissociation rates

Ca^{2+} dissociation from site II was directly monitored by mixing Ca^{2+}-loaded cTnC with an excess of a spectroscopically sensitive chelator: either Quin 2 or BAPTA. As previously demonstrated, the binding of free Ca^{2+} to both of these chelators is rapid and occurs within the deadtime of the stopped flow measurement (Nalefski et al., 1997; Peersen et al., 1997). Thus, the formation of Ca^{2+}-chelator complex observed after the deadtime represents the rate-limiting dissociation of Ca^{2+} from protein binding sites. Both of the chelators revealed that Ca^{2+} dissociation from protein was a biexponential process (not shown), in which the faster component is assigned to Ca^{2+} dissociation from the rapid signaling site II while the slow component represents the simultaneous Ca^{2+} dissociation from the cooperative, high-affinity structural sites III and IV. These assignments are confirmed by the fast (ms) and slow (s) conformational events that they trigger, which are revealed by IAANS fluorescence changes and can be directly attributed to the N- and C-terminal domains, respectively (see below).

The rate constants of Ca^{2+} dissociation and association at site II were determined as follows. For each stopped flow measurement of Ca^{2+} dissociation, the early data (beginning after the deadtime and continuing to 40 ms) were dominated by the site II dissociation and thus were well approximated by a mono-exponential fit, as illustrated in Figure 2 for cTnC-wt-IAANS using the BAPTA chelator. By contrast, the Ca^{2+} dissociation from tightly coupled sites III and IV is two-orders of magnitude slower and thus does not significantly contribute to the early data. The resulting mono-exponential early time courses yielded site II Ca^{2+} off-rates that were similar for cTnC-wt, cTnC-C35S, cTnCwt-IAANS$_2$, and cTnC-C35S-IAANS (k_{off} = 700–800 s^{-1} at 4 °C), as summarized in Table 2. These measured site II Ca^{2+} off-rates, together with the corresponding equilibrium dissociation constants (Table 1), further enabled calculation of the macroscopic site II Ca^{2+} on-rate constants from the relationship $k_{on} = k_{off}/K_D$. Again, these on-rates were similar for all four variants tested (2–4 × 10^8 M^{-1} s^{-1} at 4 °C) (Table 2). The Arrhenius activation energies of Ca^{2+} binding and dissociation could not be determined, since Ca^{2+} kinetics became too fast to measure by stopped flow at temperatures higher than 4 °C. Finally, although the indicated site II Ca^{2+} off-rate is the first measured for a cTnC protein, the calculated on-rate agrees well with the value determined for rat cTnC (k_{on} = 1.4 × 10^8 M^{-1} s^{-1} at 4 °C) (Dong et al., 1996), which shares 98% sequence identity with the chicken cTnC used in the present study.

Rates of conformational changes induced by Ca^{2+} binding and dissociation

The rates of conformational rearrangements within cTnC were monitored by IAANS fluorescence to ascertain whether or not these rearrangements occur on the same timescale as Ca^{2+} binding and dissociation at site II. Stopped flow mixing of Ca^{2+} with

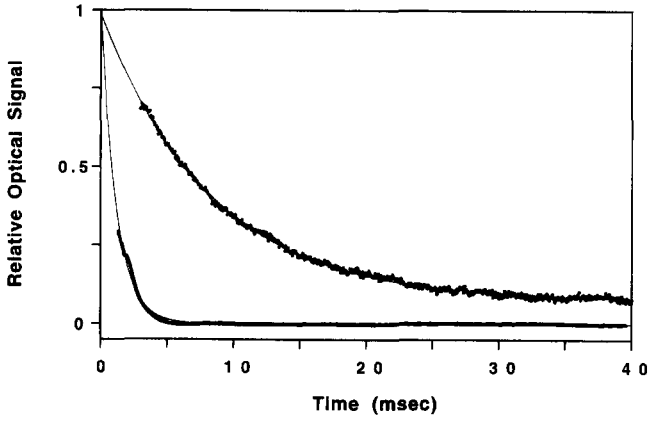

Fig. 2. Time course of Ca^{2+} dissociation from site II of cTnC-wt-IAANS$_2$ and the ensuing conformational change. Illustrated are time courses for Ca^{2+} dissociation from site II and the Ca^{2+} dissociation-induced conformational change, both for cTnC-wt-IAANS$_2$. (Upper curve) Protein conformational change was measured by mixing 2 μM protein plus 20 μM Ca^{2+} with 1 mM EDTA and monitoring the change in IAANS fluorescence. (Lower curve) Ca^{2+} dissociation was measured by mixing 12 μM protein plus 40 μM Ca^{2+} with 200 μM BAPTA in a stopped-flow spectrophotometer and monitoring the change in BAPTA absorbance. Mono-exponential curve fits yield $k_{\Delta off}$ = 90 ± 20 s^{-1} for the IAANS-detected conformational change and k_{off} = 848 ± 4 s^{-1} for the BAPTA-detected Ca^{2+} dissociation from site II (solid curves). (The minor oscillation observed in the BAPTA trace is an instrumental artifact of absorbance mode.) Conditions were 90 mM KCl, 10 mM MOPS pH 7.0, 4 °C.

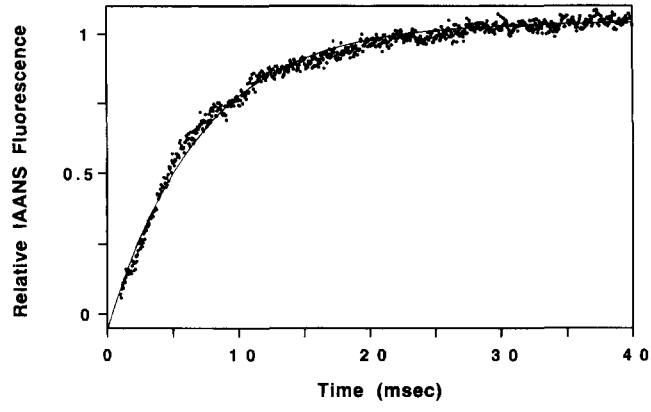

Fig. 3. Time course of the Ca^{2+}-induced conformational change for cTnC-wt-IAANS$_2$. Illustrated is the time course for conformational change upon Ca^{2+} binding to site II of cTnC-wt-IAANS$_2$. Two μM protein was rapidly mixed by stopped flow with 45 μM Ca^{2+} while monitoring the protein conformation via IAANS fluorescence. The resulting data were fitted to a mono-exponential equation, yielding the solid curve and $k_{\Delta on}$ = 150 ± 10 s^{-1}. Conditions were as in Figure 2, except that 1 mM Mg^{2+} was present to fill the Ca^{2+}/Mg^{2+}-specific sites III and IV, thereby ensuring that they do not contribute significantly to the illustrated early data.

Mg^{2+}-loaded, IAANS-labeled cTnC yields a time-dependent increase in the IAANS fluorescence intensity as shown in Figure 3. Under these conditions, the Ca^{2+}/Mg^{2+}-selective sites III and IV are loaded with Mg^{2+} and do not contribute to the early fluorescence change, while the empty Ca^{2+}-specific site II rapidly binds Ca^{2+} and triggers the conformational change detected by IAANS fluorescence. The early data (1.5 to 40 ms) are well-fit by a mono-exponential function, yielding the rate constant of the site II-associated, Ca^{2+}-triggered conformational change ($k_{\Delta on}$). This rate constant is similar, but not identical, to that for the cTnC-wt-IAANS$_2$ and cTnC-C35S-IAANS proteins ($k_{\Delta on}$ = 100–200 s^{-1} at 4 °C) and is independent of the Ca^{2+} and protein concentrations over the accessible ranges (1–2.5 μM labeled protein, 8–50 μM Ca^{2+} ion; lower, subsaturating, Ca^{2+} concentrations could not be analyzed due to insufficient signal amplitude). Significantly, the observed rates of conformational change are 8- to 200-fold slower than the calculated pseudo-first order rate of Ca^{2+} binding to site II ($k_{on}\cdot[Ca^{2+}]$). It follows that the conformational rearrangement follows Ca^{2+} binding and represents the rate-determining step in the transition from the inactive to the active state following a sudden burst of free Ca^{2+} (see Discussion).

A parallel study of rat cTnC-C35S-IAANS (Dong et al., 1996) has also measured the rate of change in IAANS fluorescence upon Ca^{2+} binding to site II. These authors observed two fast components in the IAANS fluorescence change triggered by saturating [Ca^{2+}] (>8 μM). The fastest component was [Ca^{2+}]-dependent and proposed to be the Ca^{2+} binding event at site II, while the subsequent [Ca^{2+}]-independent component was attributed to a protein conformational change that followed Ca^{2+} binding at site II. By contrast, the present results indicate that for chicken cTnC, the IAANS probe selectively detects only the latter [Ca^{2+}]-independent

Table 2. *Kinetics of Ca^{2+} binding and dissociation at site II and of the associated conformational changes*

	Calculated Ca^{2+} k_{on}[b] ($M^{-1}s^{-1}$)		IAANS $k_{\Delta on}$[c] (s^{-1})	Quin Ca^{2+} k_{off}[d] (s^{-1})	BAPTA Ca^{2+} k_{off}[d] (s^{-1})		IAANS $k_{\Delta off}$[e] (s^{-1})
Protein	Unlabeled	IAANS-labeled	IAANS-labeled	Unlabeled	Unlabeled	IAANS-labeled	IAANS-labeled
cTnC-wt	(4 ± 1) × 10^8	(2 ± 1) × 10^8	120 ± 10 (10)	772 ± 10 (67)	709 ± 27 (36)	689 ± 59 (52)	90 ± 10 (18)
cTnC-C35S	(3 ± 1) × 10^8	(2 ± 1) × 10^8	210 ± 20 (24)	779 ± 67 (36)	721 ± 38 (36)	801 ± 83 (48)	260 ± 10 (18)

[a]All samples contained 90 mM KCl, 10 mM MOPS pH 7.0, at 4 °C. Parentheses indicate the number of individual time courses analyzed.

[b]Calculated rate constant for Ca^{2+} binding to site II ($k_{on} = k_{off}/K_D$).

[c]Rate of the conformational change induced by Ca^{2+} binding to site II, determined by mixing apo IAANS-labeled protein with Ca^{2+} and monitoring IAANS fluorescence. Final was 1–5 μM protein, 1 mM Mg^{2+} to fill sites III and IV, and 8–500 μM Ca^{2+}.

[d]Rate constant for Ca^{2+} dissociation from site II, determined by mixing Ca^{2+}-loaded protein with Quin 2 or BAPTA and monitoring the change in chelator fluorescence or absorbance. Final was four μM protein, 20 μM Ca^{2+}, and 75–100 μM chelator.

[e]Rate of the conformational change induced by Ca^{2+} release from site II, determined by mixing Ca^{2+}-loaded, IAANS-labeled protein with an excess of Ca^{2+} chelator and monitoring IAANS fluorescence. Final was 1 μM protein, 5–10 μM Ca^{2+}, and 0.5–2.5 mM EDTA or BAPTA.

conformational change. The measured $k_{\Delta on}$ values are similar (within a factor of two) for chicken and rat cTnC.

Stopped flow IAANS fluorescence experiments also revealed a conformational change following Ca^{2+} dissociation from site II. When Ca^{2+}-loaded, IAANS-labeled cTnC was mixed with an excess of Ca^{2+} chelator (EDTA or BAPTA), an IAANS fluorescence decrease was triggered by Ca^{2+} dissociation from site II, as well as a much slower fluorescence increase initiated by loss of Ca^{2+} from sites III and IV. The early data (1.5 to 40 ms) were dominated by the fluorescence decrease triggered by Ca^{2+} dissociation from site II, yielding a simple, mono-exponential process as illustrated in Figure 2 for cTnC-wt-IAANS$_2$. The best-fit conformational rate constant for cTnC-wt-IAANS$_2$ or cTnC-C35S-IAANS ($k_{\Delta off}$ = 90 or 260 s^{-1}, respectively) is from threefold to eightfold slower than the rate constant for Ca^{2+} dissociation from site II (Table 2). It follows that the conformational event follows Ca^{2+} release from site II, corresponding to the relaxation of the structure from the Ca^{2+}-activated state to the inactive state. The rate constant $k_{\Delta off}$ was also measured at 25, 20, and 10 °C (data not shown), allowing determination of the Arrhenius activation energy for the inactivating conformational change (E_a = 12.3 or 9.0 kcal mol^{-1} for cTnC-wt-IAANS$_2$ or cTnC-C35S-IAANS, respectively). It should be noted that the $k_{\Delta off}$ measured here differs substantially from that previously determined (Dong et al., 1996) for rat cTnC-C35S-IAANS under different experimental conditions ($k_{\Delta off} \approx 102$ s^{-1} in 30 mM MOPS pH 7.0, 0.2 M KCl, 3 mM $MgCl_2$ at 4 °C). However, using the latter conditions, we obtained a $k_{\Delta off}$ for the chicken protein that was within error of that previously measured for rat cTnC (data not shown). Thus, the two proteins undergo similar conformational rearrangements upon removal of Ca^{2+} from site II.

Discussion

Site II of cTnC triggers heart muscle contraction by generating Ca^{2+}-induced conformational changes, and the present study seeks to elucidate the kinetic pathway for these conformational events in the purified cTnC protein. To this end, we have determined four critical rate constants for Ca^{2+} binding to site II of purified cTnC: the macroscopic Ca^{2+} on- and off-rates (k_{on}, k_{off}) and the rates of the associated conformational changes ($k_{\Delta on}$ and $k_{\Delta off}$, respectively). The fluorescent probe IAANS covalently coupled to Cys84, previously shown to sense the protein conformational change caused by Ca^{2+} binding to site II (Johnson et al., 1980; Putkey et al., 1989, 1997; Hannon et al., 1992; Howarth et al., 1995; Dong & Cheung, 1996; Dong et al., 1997a, 1997b), was used to monitor the time course of conformational rearrangement. To ensure specific labeling of Cys84, we removed the only other cysteine residue present in cTnC by the mutation C35S. Site II Ca^{2+} affinities of cTnC-wt, cTnC-C35S, cTnC-wt-IAANS, and cTnC-C35S-IAANS were measured to assess the effects of the C35S mutation and the IAANS label. The Ca^{2+} K_D is not significantly altered by either modification (Table 1), and the rates of Ca^{2+} binding or dissociation at site II are similar for all four cTnC variants examined (Table 2). Thus, the thermodynamics and kinetics of Ca^{2+} binding to site II are relatively unperturbed by the C35S mutation and by IAANS labeling.

Previous studies have suggested that binding of Ca^{2+} to the trigger sites of cardiac and skeletal troponin C and the Ca^{2+}-induced conformational change may occur as separate steps. It has been inferred (Dong et al., 1996) that Ca^{2+} binding to site II of cTnC could occur at a faster rate than the Ca^{2+}-induced conformational change. Other studies have examined Ca^{2+} dissociation from the related protein skeletal troponin C (sTnC) using the fluorescent Ca^{2+} chelator Quin 2. In the sTnC protein, Ca^{2+} appears to dissociate from the N-terminal domain regulatory domain somewhat more rapidly than the dansyl-detected protein conformational change, although the difference between rate constants is subtle (Johnson et al., 1994). The present work directly tests the hypothesis that cTnC activation and inactivation are two-step events by comparing under identical conditions the time courses of both (1) Ca^{2+} dissociation from cTnC site II as monitored by Ca^{2+} chelators, and (2) conformational changes as detected by IAANS fluorescence. The results demonstrate that in the case of isolated cTnC, both the activation and inactivation processes involve a fast Ca^{2+} equilibration event followed by a slow conformational transition.

A kinetic cycle that adequately describes our data for isolated cTnC is illustrated in Figure 4. In this scheme, all the microscopic steps are reversible and only the Ca^{2+} binding, Ca^{2+} dissociation, and conformational steps involving site II are considered. The upper branch corresponds to the cTnC activation by a Ca^{2+} burst that would lead to heart contraction, while the lower branch represents the transition back to the inactive, relaxed state after the Ca^{2+} transient. Most of the microscopic rate constants are defined by the present results.

The stopped flow experiment that mixes the Ca^{2+}-saturated protein with excess Ca^{2+} chelator drives the system along the lower branch of the cycle that converts the activated conformation (cTnC*) to the inactive conformation (cTnC):

$$\text{cTnC*}\cdot Ca^{2+} \xrightarrow{k_3} \text{cTnC*} + Ca^{2+} \xrightarrow{k_4} \text{cTnC} + Ca^{2+} \qquad (1)$$

where the reverse reactions are neglected because free Ca^{2+} is immediately trapped by the chelator. In this two-step reaction, the rate of Ca^{2+} dissociation from site II measured by a chelator optical signal ($k_3 \equiv k_{off}$ = 700–800 s^{-1}) is observed to be signif-

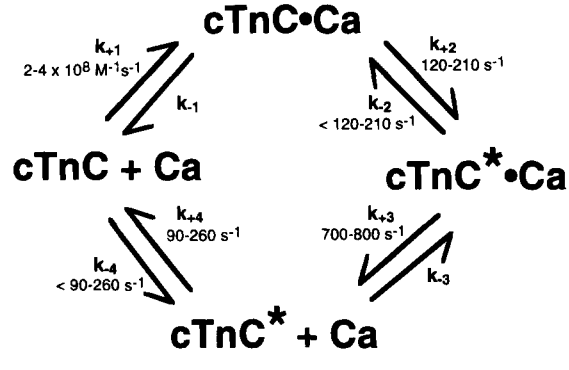

Fig. 4. Kinetic model for the Ca^{2+} binding and conformational events at site II of cTnC. Each discrete event involving Ca^{2+} binding or dissociation at site II, or a site II-triggered conformational change, is denoted by a microscopic rate constant. The transition of the protein conformation between the inactive state (cTnC) and the active state (cTnC*) is detected as a fluorescence change of the protein-coupled probe IAANS. Shown for each rate constant is the range of values determined for two related proteins: chicken cTnC-wt-IAANS$_2$ and cTnC-C35S-IAANS. Experimental conditions were 90 mM KCl, 10 mM MOPS pH 7.0, 4 °C. The indicated macroscopic k_{+1} closely matches the microscopic value measured at 4 °C for the highly homologous rat cTnC-C35S-IAANS under similar conditions (1.4×10^8 M^{-1} s^{-1}) (Dong et al., 1996).

icantly faster than the rate of conformational change measured by a fluorophore coupled to the protein ($k_4 \equiv k_{\Delta off} = 90–260\ s^{-1}$). Both the first step ($k_3$) and the second step ($k_4$) yield simple mono-exponential kinetics with different rate constants, as expected for a sequential reaction in which the slow second step is rate determining. Measurement of k_4 also provides an upper limit on the reverse rate constant k_{-4} in Figure 4, since, in the absence of Ca^{2+}, the equilibrium favors the inactive conformation ($K = k_4/k_{-4} > 1$).

A second stopped flow experiment that mixes apo site II with saturating Ca^{2+} drives the system along the upper branch of the kinetic cycle toward the activated state:

$$cTnC + Ca^{2+} \overset{k_1}{\rightleftharpoons} cTnC \cdot Ca^{2+} \overset{k_2}{\longrightarrow} cTnC^* \cdot Ca^{2+} \qquad (2)$$

where it is assumed that the reverse of the second step is negligible due to the greater stability of the activated conformation in the Ca^{2+}-occupied state. The second order rate constant for Ca^{2+} binding has been measured for the nearly identical rat cTnC protein ($k_1 = 1.4 \times 10^8\ M^{-1}\ s^{-1}$) (Dong et al., 1996) and is similar to the macroscopic Ca^{2+} on-rate determined in this study ($k_{on} = 2–4 \times 10^8\ M^{-1}\ s^{-1}$). For the Ca^{2+} concentrations used here, the rate of the Ca^{2+} binding step is 1,600–20,000 events s^{-1} ($= k_1 \cdot [Ca^{2+}]$), which is too fast to be preceded by the slow conformational change to the activated state ($k_{-4} < 90–260\ s^{-1}$; see above). It follows that Ca^{2+} binds primarily to the inactive conformation of the apo protein as shown in Equation 2, and that this binding event is followed by the slow conformational transition to the activated state as detected by the protein-coupled IAANS fluorophore ($k_2 \equiv k_{\Delta on} = 120–210\ s^{-1}$). The simple mono-exponential kinetics observed for this conformational step are consistent with the proposed two-step reaction, since such kinetics are expected for product formation when the second step is rate-determining. (Note that additional steps, such as a fast conformational step (Dong et al., 1996) within the k_1 event, may be present but concealed by the rate determining step.) Finally, the measured value of k_2 places an upper limit on the reverse rate constant k_{-2}, since the equilibrium favors the active conformation in the Ca^{2+}-loaded state (Fig. 4).

We emphasize that the experiments described herein have determined equilibrium and kinetic parameters for the isolated cTnC molecule, thereby providing a set of baseline parameters against which the properties of cTnC can be compared in multi-protein systems. The Ca^{2+} binding and conformational features of cTnC are known to change upon complexation with other proteins involved in muscle contraction (Holroyde et al., 1980; Iio & Kondo, 1982; Rosenfeld & Taylor, 1985; Dong et al., 1997b; Putkey et al., 1997). For example, IAANS fluorescence studies suggest that the kinetics of Ca^{2+}-induced conformational changes are significantly slowed when cTnC is incorporated into the full troponin complex (Dong et al., 1997b). Furthermore, IAANS-labeled cTnC reconstituted into muscle fibers is able to detect perturbations due to myosin-induced cooperativity or crossbridge formation (Hannon et al., 1992; Putkey et al., 1997). Of special interest are the rates of Ca^{2+}-induced conformational changes for cTnC within the intact muscle fiber, since these rates include all of the important interactions and presumably define the activation and inactivation parameters of heart muscle contraction. Given the present results, it is reasonable to propose that certain cTnC-regulated events during heart contraction and relaxation may well involve a rapid Ca^{2+} equilibration step followed by a slow conformational transition.

Comparison of the data in Tables 1 and 2 demonstrates that modifications at residue Cys35 in vestigial site I affect the kinetics of conformational changes triggered by site II, even though the Ca^{2+} on- and off-rates at site II are not substantially altered. In particular, the conformational change rates $k_2 \equiv k_{\Delta on}$ and $k_4 \equiv k_{\Delta off}$ are each twofold to threefold slower, and the Arrhenius activation energy for the latter reaction is 3 kcal mol^{-1} higher, for cTnC-wt-IAANS$_2$ than for cTnC-C35S-IAANS. The most likely explanation for this difference is that the bulky IAANS probe at position Cys35 increases the activation barrier for the conformational change, thereby slowing the rate of conformational change in both the forward and reverse directions without perturbing the overall equilibrium. The conservative serine substitution at position 35, by contrast, presumably has little or no effect. In this picture, the conformational kinetics of cTnC-wt-IAANS$_2$ are consistently slower than those of cTnC-C35S-IAANS because the former protein possesses the bulky IAANS label at position 35.

The Cys35 residue is located in vestigial site I of cTnC, a region previously implicated in Ca^{2+} signaling. Fluorescence polarization experiments using engineered tryptophan residues, for example, have suggested that vestigial site I of cTnC is locked in an activated state, while site I from sTnC requires Ca^{2+} to achieve the same conformation (Rao et al., 1995). Furthermore, sTnC is unable to regulate muscle contraction in skinned muscle fibers when site I is inactivated by mutagenesis, but replacement of inactive sTnC site I with the N-terminal portion of cTnC containing vestigial site I restores regulation of muscle contraction (Gulati et al., 1992). Recent work demonstrates that the environment of Cys35-IAANS becomes less polar and less solvent-exposed when apo cTnC is incorporated into the troponin complex, while the environment of Cys84-IAANS remains essentially unchanged (Dong et al., 1997a; Putkey et al., 1997), suggesting that vestigial site I is in close contact with the troponin complex where it could have an important impact on transmittance of signal. The present effects of Cys35 modification on the conformational kinetics of cTnC support the conclusion that vestigial site I represents a critical region for activation of muscle contraction.

Materials and methods

Protein expression and purification

Expression plasmids encoding wild-type chicken cTnC (cTnC-wt) and the engineered cTnC derivative (cTnC-C35S) have been described (Putkey et al., 1989, 1993). Codons for the first ten amino acids of cTnC were altered so they would better conform to bacterial codons, thus increasing bacterial protein expression. One mutation, D2A, was introduced by this alteration. The cTnC gene is located behind the λ-pL promoter, allowing protein expression in the absence of the λ-cI repressor. The host *E. coli* strain used for protein expression, strain GW contains the cI-857 temperature-sensitive repressor, which is fully functional at 30 °C but is inactivated at 42 °C, allowing cTnC expression. Using this expression system, cTnC was produced and isolated as previously described (Putkey et al., 1989). Briefly, Luria broth containing 100 mM ampicillin was inoculated with 0.01 volume of overnight culture. The cells were grown at 30 °C to an OD_{600} of ~1.0. The temperature was then shifted to 42 °C and protein production was induced for 2 h. Whole cells analyzed by SDS-polyacrylamide gel electrophoresis exhibited an intense band at ~18 kDa (the molecular weight of cTnC), which was absent in uninduced cells. The cells were har-

vested by spinning at 9,500 rpm for 15 min at 4 °C, and the pellet was frozen at −70 °C until use. After thawing, cells were resuspended in 50 mM Tris, pH 7.5, 0.2 mM EDTA (DEAE loading buffer) and French pressed twice. Lysed cells were spun in a TL100 centrifuge at 80,000 rpm (350,000 *g*) for 15 min to pellet cell debris. The supernatant was loaded onto a DEAE Sephadex A-25 column pre-equilibrated with DEAE loading buffer. After the protein was loaded, two column volumes of buffer were washed through the column. The protein was eluted with a 300 mL linear gradient of 0 to 0.75 M KCl in DEAE loading buffer. The presence of cTnC was determined using SDS-polyacrylamide gel electrophoresis. Fractions containing cTnC were pooled, and the pooled fractions were concentrated to less than 10 mL using a YM10 membrane in an Amicon concentration device. The protein was then dialyzed against four changes of 10 mM MOPS, pH 7.5, 90 mM KCl, two mM $CaCl_2$. When analyzed by SDS-polyacrylamide gel electrophoresis, the protein was generally ~90% pure.

Protein analysis

Protein concentration of a stock solution of cTnC was determined using the tyrosinate difference spectral method (Copeland, 1994), and this stock solution was used to standardize the Bradford protein assay. In all calculations, the protein concentration was corrected for purity, as determined by SDS polyacrylamide gel electrophoresis. The identities and homogeneity of both cTnC-wt and cTnC-C35S were confirmed by measurement of their molecular masses using a Sciex API-III triple quadrupole electrospray mass spectrometer directly coupled to liquid chromatographic separation (LC/MS), as described elsewhere (Drake & Falke, 1995). Ca^{2+} binding stoichiometries were determined using flow dialysis methodology (Peersen et al., 1997)

Labeling of cTnC with IAANS

The fluorescent probe IAANS was reacted with cTnC as described previously (Johnson et al., 1980). A fivefold molar excess of IAANS was added to 50 mM protein in 10 mM MOPS, pH 7.5, 90 mM KCl, two mM $CaCl_2$. Labeling reactions, kept in the dark, were incubated 1–3 h at room temperature. Labeling stoichiometry was determined based on an extinction coefficient at 325 nM of 24,900 M^{-1} cm^{-1} (Johnson et al., 1980).

Removal of Ca^{2+} and excess label from protein samples

The buffer used in the following purification protocol was 10 mM MOPS, pH 7.0, 90 mM KCl. All plasticware and cuvettes were treated with EDTA and thoroughly rinsed before use. Excess IAANS label and Ca^{2+} was removed in two steps. In the first purification step, the protein was run through a Sephadex G10 centrifuge column (Penefsky, 1977). To make the centrifuge column, a Biorad Econo-column was filled to the 2 mL mark with pre-swollen Sephadex G10, and the resin was equilibrated with 10 mL of buffer. The column was placed in a conical tube and spun for 2 min in a JA20 rotor at 1,500 rpm (272 *g*) to remove excess liquid. After moving the pre-spun column into a clean conical tube, 1 mL of cTnC sample was loaded, and the spin was repeated to elute the protein. The cTnC elutes rapidly from the column in the void volume, while small molecules (Ca^{2+} and IAANS) remain in the column bed. Protein recovery was 90–100%. In the absence of protein, 99.7% of IAANS was removed from buffer based on absorbance measurements at 325 nM. In the second purification step, the protein was loaded onto a 0.5 mL Chelex column and eluted with approximately two volumes of buffer. Overall protein recovery through both purification steps was ~60%.

Equilibrium fluorescence measurements

IAANS and magnesium green fluorescence were monitored using an SLM instruments 48000 S fluorimeter. Excitation and emission wavelengths were 325 and 450 nM, respectively, for IAANS, and 506 and 532 nM for magnesium green (excitation bandpass = 4 nM, emission bandpass = 8 nM). Protein samples and EGTA, magnesium green and Ca^{2+} stock solutions were in 10 mM MOPS, pH 7.0, 90 mM KCl. Stirred methacrylate cuvettes containing 1–5 μM protein were thermostatted to 4 or 25 °C, and EGTA, magnesium green, and Ca^{2+} were added from concentrated stock solutions as indicated.

Measurement of Ca^{2+} K_D using IAANS fluorescence

Ca^{2+} was titrated with cTnC-IAANS in the presence of 1 mM EGTA, and the fluorescence emission signal at 450 nM was monitored as described above. $[Ca^{2+}]_{free}$ was calculated based on dilution-corrected $[Ca^{2+}]_{total}$ and [EGTA] using the program Chelator (Schoenmakers et al., 1992), which takes into account ionic strength, buffer, and temperature conditions. The fluorescence of IAANS attached to Cys84 decreases upon Ca^{2+} binding to tightly coupled sites III and IV, and increases upon Ca^{2+} binding to site II (Johnson et al., 1980). Thus, a two-component binding formula, Equation 3, was best-fit to the fluorescence titration data by KaleidaGraph 3.0 software for the Macintosh (Synergy Software, Reading, Pennsylvania):

$$F = \frac{\Delta F_1}{1 + 10^{(\log K_{D(\mathrm{III,IV})} - \log[Ca^{2+}]_{free})}} + \frac{\Delta F_2}{1 + 10^{(\log K_{D(\mathrm{II})} - \log[Ca^{2+}]_{free})}} \quad (3)$$

where ΔF_1 and ΔF_2 represent the maximum negative and positive change in fluorescence intensity, respectively, from which the corresponding Ca^{2+} dissociation constants for sites III and IV ($K_{D(\mathrm{III,IV})}$) and for site II ($K_{D(\mathrm{II})}$) are determined.

Measurement of Ca K_D using the fluorescent chelator magnesium green

The methodology described here for measurement of protein Ca^{2+} K_D using the fluorescent Ca^{2+} chelator magnesium green is based on previously described methodologies (Linse et al., 1991a, 1991b; Bryant, 1985). The magnesium green Ca^{2+} K_D was determined by titrating the Ca^{2+}-induced change in magnesium green fluorescence as described above, which enabled Equations 4–6 to be solved simultaneously. Equations 4 and 5 describe $[Ca^{2+}]_{free}$:

$$[Ca^{2+}]_{free} = \frac{K_D(F - F_{min})}{(F_{max} - F)} \quad (4)$$

$$[Ca^{2+}]_{free} = [Ca^{2+}]_{total} - \Sigma[Ca^{2+}]_{bound}. \quad (5)$$

Equation 4 relates $[Ca^{2+}]_{free}$ to fluorescence at a given point in the titration (F) based on the fluorescence maximum (F_{max}), the fluorescence minimum (F_{min}), and the Ca^{2+} K_D. Equation 5 describes the distribution of Ca^{2+} in the presence of one or more Ca^{2+} binding molecules, in this case, magnesium green only. $[Ca^{2+}]_{total}$ is the sum of $[Ca^{2+}]_{free}$ plus the concentration of Ca^{2+} contamination present at the beginning of the titration. The concentration of Ca^{2+} bound to magnesium green ($[Ca^{2+}]_{bound \cdot Mg\ green}$) can be described by Equation 6,

$$[Ca^{2+}]_{bound \cdot Mg\ green} = \frac{[\text{Mg green}](F - F_{min})}{(F_{max} - F_{min})} \quad (6)$$

where [Mg green] is the total concentration of magnesium green, which is determined spectroscopically (ϵ = 75,200 M^{-1} cm^{-1} at 506 nM). The Microsoft Excel Solver function was used to minimize the error square sum between the two solutions for $[Ca^{2+}]_{free}$ at each step in the titration using Equations 4–6 by varying the Ca^{2+} K_D and initial concentration of contaminating Ca^{2+}. Solutions for Ca^{2+} K_D were found to be independent of the initial guess. Magnesium green Ca^{2+} K_D of 6.1 ± 0.3 and 7.0 ± 0.4 μM were determined at 25 and 4 °C, respectively.

Ca^{2+} K_D of protein samples was determined by titrating the Ca^{2+}-induced change in magnesium green fluorescence in the presence of equimolar protein (2–5 μM) and solving Equations 4–7. Equations 4 and 6 enable determination of $[Ca^{2+}]_{free}$ and $[Ca^{2+}]_{bound \cdot Mg\ green}$, respectively. Equation 5 is solved for $[Ca^{2+}]_{bound \cdot cTnC}$ ($= [Ca^{2+}]_{total} - [Ca^{2+}]_{free} - [Ca^{2+}]_{bound \cdot Mg\ green}$), which can also be described by Equation 7:

$$[Ca^{2+}]_{bound \cdot cTnC} = [\text{cTnC}] \frac{\Sigma(n*[Ca^{2+}]_{free})}{([Ca^{2+}]_{free} + K_D)} \quad (7)$$

where [cTnC] is the total concentration of cTnC and n is the binding stoichiometry. The Microsoft Excel Solver function was used to minimize the error square sum between the two solutions for $[Ca^{2+}]_{bound \cdot cTnC}$ at each step in the titration by changing the Ca^{2+} K_D of site II and the initial $[Ca^{2+}]_{free}$. The Ca^{2+} K_D values of sites III and IV were assumed to be K_D = 0.2 μM (the macroscopic $K_{D(II,III)}$ determined by IAANS titration for these two tightly coupled sites), since both of these sites were essentially Ca^{2+}-saturated at the beginning of the titration.

Stopped flow experiments

cTnC protein was rapidly mixed with Ca^{2+} or a Ca^{2+}-chelator (Quin 2, BAPTA or EDTA) in an Applied Photophysics SX17MV stopped flow fluorimeter (acquisition time = 0.5–1 s, 4,000 data points collected). In Quin 2-monitored experiments, fluorescence was excited using a wavelength of 347 nM, while emission was collected by placing a 490 nM bandpass filter between the observation cell and the detector, oriented perpendicular to the excitation beam. In IAANS-monitored experiments, fluorescence was excited using a 325 nM excitation beam and the resulting emission was collected via a 335 nM high pass filter. BAPTA absorbance was monitored at both absorbance maxima (253 and 276 nM). The instrumental deadtimes were 0.9 s (fluorescence detection mode, 2 mm pathlength) and 1.3 s (absorbance mode, 10 mm path). Additional details are described elsewhere (Nalefski et al., 1997; Peersen et al., 1997).

Acknowledgments

Funding for this research was provided by the National Institutes of Health (grants GM48203 to JJF, HL09225 to ALH, HL45724 to JAP) and by the Robert Welch Foundation (grant AU1144 to JAP). We thank Dr. Albert Gordon (University of Washington) for helpful comments.

References

Babu YS, Bugg CE, Cook WJ. 1988. Structure of calmodulin refined at 2.2 Å resolution. *J Mol Biol 204*:191–204.

Bryant DTW. 1985. Quin 2: The dissociation constants of its Ca^{2+} and Mg^{2+} complexes and its use in a fluorimetric method for determining the dissociation of Ca^{2+}-protein complexes. *Biochem J 226*:613–616.

Burtnick LD, Kay CM. 1977. Ca^{2+} binding to cardiac troponin C. *FEBS Lett 75*:105–110.

Chattopadhyaya R, Meador WE, Means AR, Quiocho FA. 1992. Calmodulin structure refined at 1.7 Å resolution. *J Mol Biol 228*:1177–1192.

Copeland RA. 1994. *Methods for protein analysis*. New York: Chapman and Hall.

Dong WJ, Cheung HC. 1996. Calcium-induced conformational change in cardiac troponin C studied by fluorescence probes attached to cys-84. *Biochim Biophys Acta 1295*:139–146.

Dong WJ, Rosenfeld SS, Wang CK, Gordon AM, Cheung HC. 1996. Kinetic studies of calcium binding to the regulatory site of troponin C from cardiac muscle. *J Biol Chem 271*:688–694.

Dong WJ, Wang CK, Gordon AM, Cheung HC. 1997a. Disparate fluorescence properties of 2-[4′(iodoacetamido)anilino]-naphthalene-6-sulfonic acid attached to Cys84 and Cys35 of troponin C in cardiac muscle troponin. *Biophys J 72*:850–857.

Dong WJ, Wang CK, Gordon AM, Rosenfeld SS, Cheung HC. 1997b. A kinetic model for the binding of Ca^{2+} to the regulatory site of troponin from cardiac muscle. *J Biol Chem 272*:19229–19235.

Dotson DG, Putkey JA. 1993. Differential recovery of Ca^{2+} binding activity in mutated EF-hands of cardiac troponin C. *J Biol Chem 268*:24067–24073.

Drake SK, Falke JJ. 1996. Kinetic tuning of the EF-hand calcium binding motif: The gateway residue independently adjusts (i) barrier height and (ii) equilibrium. *Biochemistry 35*:1753–1760.

Finn BE, Evenas J, Drakenberg T, Waltho JP, Thulin E, Forsen S. 1995. Calcium-induced structural changes and domain autonomy in calmodulin. *Nature Struct Biol 2*:777–783.

Gagne SM, Tsuda S, Li MX, Smillie LB, Sykes BA. 1995. Structures of the troponin C regulatory domains in the apo and calcium-saturated states. *Nature Struct Biol 2*:784–789.

Gulati J, Babu A, Putkey JA. 1989. Down-regulation of fast-twitch skeletal muscle fiber with cardiac troponin-C and recombinant mutants. *FEBS Lett 248*:5–8.

Gulati J, Babu A, Su H. 1992. Functional delineation of the Ca^{2+}-deficient EF-hand in cardiac muscle, with genetically engineered cardiac-skeletal chimeric troponin C. *J Biol Chem 267*:25073–25077.

Hannon JD, Martyn DA, Gordon AM. 1992. Effects of cycling and rigor crossbridges on the conformation of cardiac troponin C. *Cir Res 71*:984–991.

Herzberg O, James MNG. 1988. Refined crystal structure of troponin C from turkey skeletal muscle at 2.0 Å resolution. *J Mol Biol 203*:761–779.

Holroyde MJ, Robertson SP, Johnson JD, Solaro RJ, Potter JD. 1980. The calcium and magnesium binding sites of cardiac troponin and their role in the regulation of myofibrillar adenosine triphosphatase. *J Biol Chem 255*:11688–11693.

Howarth JW, Krudy GA, Lin X, Putkey JA, Rosevear PR. 1995. An NMR and spin label study of the effects of binding calcium and troponin I inhibitory peptide to cardiac troponin C. *Protein Sci 4*:671–680.

Iio T, Kondo H. 1982. Fluorescence titration and fluorescence stopped-flow studies on skeletal muscle troponin labeled with fluorescence reagent. *J Biochem 92*:1141–1149.

Johnson JD, Collins JH, Robertson SP, Potter JD. 1980. A fluorescent probe study of Ca^{2+} binding to the Ca^{2+}-specific sites of cardiac troponin and troponin C. *J Biol Chem 255*:9635–9640.

Johnson JD, Nakkula RJ, Vasulka C, Smillie LB. 1994. Modulation of Ca^{2+} exchange with the Ca^{2+}-specific regulatory sites of troponin C. *J Biol Chem 269*:8919–8923.

Krudy GA, Kleerekoper Q, Guo X, Howarth JW, Solaro RJ, Rosevear PR. 1994. NMR studies delineating spatial relationships within the cardiac troponin I-troponin C complex. *J Biol Chem 269*:23731–23735.

Kuboniwa H, Tjandra N, Grzesiek S, Ren H, Klee CB, Bax A. 1995. Solution structure of calcium-free calmodulin. *Nature Struct Biol 2*:768–776.

Leavis PC, Kraft EL. 1978. Calcium binding to cardiac troponin C. *Arch Biochem Biophys 186*:411–415.

Liao R, Wang CK, Chueng HC. 1994. Coupling of calcium to the interaction of troponin I with troponin C from cardiac muscle. *Biochemistry 33*:12729–12734.

Lin X, Krudy GA, Howarth J, Brito RMM, Rosevear PR, Putkey JA. 1994. Assignment and calcium dependence of methionyl eC and eH resonances in cardiac troponin C. *Biochemistry 33*:14434–14442.

Linse S, Helmersson A, Forsen S. 1991a. Calcium binding to calmodulin and its globular domains. *J Biol Chem 266*:8050–8054.

Linse S, Johansson C, Brodin P, Grundstrom T, Drakenberg T, Forsen S. 1991b. Electrostatic contributions to the binding site of Ca^{2+} in calbindin D_{9k}. *Biochemistry 30*:154–162.

McCubbin WD, Kay CM. 1985. Trypsin digestion of bovine cardiac troponin C in the presence and absence of calcium. *Can J Cell Biol 63*:812–823.

Nalefski EA, Slazas MM, Falke JJ. 1997. Ca^{2+}-signaling cycle of a membrane-docking C2 domain. *Biochemistry 36:*12011–12018.

Negele JC, Dotson DG, Liu W, Sweeney HL, Putkey JA. 1992. Mutation of the high affinity calcium binding sites in cardiac troponin C. *J Biol Chem 267*:825–831.

Peersen OB, Madsen TS, Falke JJ. 1997. Intermolecular tuning of calmodulin by target peptides and proteins: Differential effects on Ca^{2+} binding and implications for kinase activation. *Protein Sci 6*:794–807.

Penefsky HS. 1977. Reversible binding of P_i by beef heart mitochondrial adenosine triphosphatase. *J Biol Chem 252*:2891–2899.

Putkey JA, Dotson DG, Mouawad P. 1993. Formation of inter- and intramolecular disulfide bonds can activate cardiac troponin C. *J Biol Chem 268*:6827–6830.

Putkey JA, Liu W, Lin X, Ahmed S, Zhang M, Potter JD, Kerrick WGL. 1997. Fluorescence probes attached to Cys35 or Cys84 in cardiac troponin C are differentially sensitive to Ca^{2+}-dependent events *in vitro* and *in situ*. *Biochemistry 36*:970–978.

Putkey JA, Sweeney HL, Campbell ST. 1989. Site-directed mutation of the trigger calcium-binding sites in cardiac troponin C. *J Biol Chem 264*:12370–12378.

Rao ST, Wu S, Satyshur KA, Ling KY, Kung C, Sundaralingam M. 1993. Structure of *Paramecium tetrauelia* calmodulin at 1.8 Å resolution. *Protein Sci 2*:436–447.

Rao VG, Akella AB, Su H, Gulati J. 1995. Molecular mobility of the Ca^{2+}-deficient EF-hand of cardiac troponin C as revealed by fluorescence polarization of genetically inserted tryptophan. *Biochemistry 34*:562–568.

Rosenfeld SS, Taylor EW. 1985. Kinetic studies of calcium binding to regulatory complexes from skeletal muscle. *J* Biol Chem 260:252–261.

Satyshur KA, Rao ST, Pyzalska D, Drendel W, Greaser M, Sundaralingam M. 1988. Refined structure of chicken skeletal muscle troponin C in the two-calcium state at 2-Å resolution. *J Biol Chem 263*:1628–1647.

Schoenmakers TJM, Visser GJ, Flik G, Theuvenet APR. 1992. Chelator: An improved method for computing metal ion concentrations in physiological solutions. *Biotechniques 12*:870–879.

Sia SK, Li MX, Spyracopoulos L, Gagné SM, Liu W, Putkey JA, Sykes BD. 1997. Structure of cardiac troponin C unexpectedly reveals a closed regulatory domain. *Biochemistry 272*:18216–18221.

Starovasnik MA, Su DR, Beckingham K, Klevit RE. 1992. A series of point mutations reveal interactions between the calcium-binding sites of calmodulin. *Protein Sci 1*:245–253.

Sweeney HL, Brito RMM, Rosevear PR, Putkey JA. 1990. The low-affinity Ca^{2+} binding sites in cardiac/slow skeletal muscle troponin C perform distinct functions: Site I alone cannot trigger contraction. *Proc Nat Acad Sci USA 87*:9538–9542.

Taylor DA, Sack JS, Maune JF, Beckingham K, Quiocho FA. 1991. Structure of a recombinant calmodulin from *Drosophila melanogaster* refined at 2.2 Å resolution. *J Biol Chem 266*:21375–21380.

van Eerd JD, Takahashi K. 1975. The amino acid sequence of bovine cardiac troponin-C. Comparison with rabbit skeletal troponin-C. *Biochem Biophys Res Comm 64*:122–127.

Zhang M, Tanaka T, Ikura M. 1995. Calcium-induced conformational transition revealed by the solution structure of apo calmodulin. *Nature Struct Biol 2*:758–767.

Zot HG, Potter JD. 1982. A structural role for the Ca^{2+}-Mg^{2+} sites on troponin C in the regulation of muscle contraction. *J Biol Chem 257*:7678–7683.